

Effect of Manganese Additions and Wear Parameter on the Tribological Behaviour of NFGrey (8) Cast Iron

J.O. Agunsoye^a, E.F. Ochulor^a, S.I. Talabi^a, S. Olatunji^a

^aDepartment of Metallurgical and Materials Engineering, University of Lagos, Akoka, Yaba, Lagos.

Keywords:

Wear
Microstructure
Carbon equivalent
Interaction effect
Hardness

ABSTRACT

The effect of manganese and wear parameter on the abrasive wear behaviour of NFGREY8 cast iron composition under dry lubrication conditions was investigated. The wear parameters studied are sliding speed, applied load, time and percentage of ferro-manganese additions. The experimental data were taken in a controlled way. Scanning electron microscope was used to examine the morphology of the samples. The results from linear regression equation and analysis of variances (ANOVA) shows that manganese additions, load and speed variable are more pronounced on the wear behaviour of the NFGrey (8) cast iron. The result showed that the additions of the 75 % ferro manganese grade decreases the carbon equivalent CE and fortify the matrix with the formation of tough $(FeMn)_3C$ inter-metallic leading to increased wear resistance of the examined composition.

Corresponding author:

J.O. Agunsoye
Department of Metallurgical and
Materials Engineering,
University of Lagos,
Akoka, Yaba, Lagos
E-mail: jagunsoye@unilag.edu.ng

© 2012 Published by Faculty of Engineering

1. INTRODUCTION

Abrasive wear of materials is fundamentally technical and economically important. The effects of several alloying elements have been studied mainly on the mechanical properties of grey cast iron [1,10-12]. Grey cast iron, which traditionally contains 2.5–5 % C and 0.8–3 % Si, is the commonly used material in machinery manufacturing [8]. The properties of grey cast iron primarily depend on its composition which is influenced by both the normal elements present in plain irons such as carbon, silicon, phosphorus, sulfur and manganese, and the presence of alloying additions and other trace

elements [7]. In alloy cast iron, the graphite morphology can be divided into three types: flake-like, vermicular-like and spherical-like. Other factors that influence the properties of cast iron include the chemical composition of the matrix, and the size, distribution, volume fraction and morphology of the individual microstructural constituents [8].

The alloying elements can modify the matrix microstructure, graphite morphology and mechanical properties of alloy cast iron. While the graphite enhances the desirable properties of cast iron, the flakes disrupt the crystal structure and precipitate cracks, leading to cast

iron's characteristic brittleness [13]. This characteristic property has limited the scope of cast application. Elements which reduce the solubility of carbon in the liquid state increase the potential of forming graphite.

Attempt had been made by researcher to widen the scope of cast Iron use. Niobium addition to grey cast iron has been found to effectively enhanced cast Iron hardness and wear resistance due to the formation of niobium-rich hard phase [1]. Reductions in the level of excess manganese significantly increased tensile strength and hardness and progressively promoted fine, mesh and spiky forms of graphite in the structure, also pearlite instead of ferrite; the pearlite became less uniform and more mixed, with coarse and fine forms [14]. It also leads to the formation of compacted graphite (as a result of reduced sulphur content) which tends to improve strength and thermal conductivity of the casting. The temperature for the start of this transformation in a base Fe-C-Si alloy is decreased by small addition of Mn or Cu. Carbides formation in cast irons may be present in the form M_3C , or M_7C_3 . These carbides may occur as lamellar, rod, or continuous matrix [8].

In unalloyed cast iron, Fe_3C either develops into a lamellar manner or forms a continuous phase. Any graphite present in the structure leads to mottled appearance. The carbide phases impart considerable hardness, wear and abrasion resistance. Similarly, Boron extends the usefulness of grey cast iron by uniformly distributing the hard particles of cementite throughout the soft matrix of grey cast iron even in certain types of chilled castings [15] as well as improves the wear characteristic of grey cast iron [2]. The addition of nickel refines the pearlite and graphite structure of grey cast iron and improves toughness and evens out hardness differences between section thicknesses. Addition of SiC instead of FeSi as a silicon carrier affects variations in the thermal analysis characteristics and microstructure together with increasing fluidity as well as decreasing chill depth [3].

High hardness of white cast iron bars produced by addition of sodium chloride salt to grey cast iron is recommended for wear resistance application [9]. There is therefore the need to exploit the possibility of using grey cast Iron for

wear application in areas where the level of impact is considered low by appropriate Ferro manganese addition and wear characterization.

2. MATERIALS AND METHOD

2.1 Material Preparation

The NFGrey (8) cast iron has been used in this study. The alloy composition used for the control sample is 3.32 % C, 1.90 % Si, 0.31 % Mn, 0.12 % P, 0.11 % S, 94.24 % Fe; the samples were sand cast in a captive foundry in Lagos, Nigeria, with a 40 kg capacity crucible furnace.

2.2 Method

Two-number wooden patterns dimension (11.50 x 11.50 x 202) mm rectangular shaped were used to make five pair of cope and drag moulds as shown in Plate A. The mouldings sand were prepared from a mixture of dried fresh silica sand, water, bentonite and dextrin in accordance with BS14 standard [17]. The five pairs of mould were labelled as Batch 1, 2, 3, 4 and 5 respectively. 10 Kg known quantity of grey cast Iron foundry returns were melted in a 40 kg capacity crucible furnace as shown in Plate B and poured at 1270 °C into improvised moulds. The first batch which represents the control sample was poured into the mould labelled batch 1 without any alloy addition as shown in Plate C. Thereafter, a known quantity of 75 % Ferro manganese granules were added to the remaining molten bath and heated up to 1282 °C, stirred manually with a dry wooden stick to facilitate a homogeneous bath and poured into the second mould labelled batch 2. This process was repeated for the remaining three batches of moulds with increasing 75 % Ferro manganese granule additions. After pouring, the castings were allowed to solidify and cooled in the mould to room temperature (36 °C) before they were carefully knock out, wire brushed to remove fused sand grain and gating system. The cast bars in Plate D were carefully fettled to the required dimension (11 x 11 x 200) mm and labelled to ensure traceability. From the cast bars (11 x 11 x 200) mm, sample representatives from each bar were cut taken and machined to standard charpy impact coupon, coupon of wear, Brinell hardness, and SEM test respectively.



Plate A. Improvised mould.



Plate B. The 40 kg crucible furnace.



Plate C. Pouring into the mould



Plate D. Sample of knockout cast.

Samples are taken for compositional analysis from the five batches of casting produced. The

results of the spectrometric analysis of the samples carried out with Hilger Analytical Direct Optical Light Emission Polyvac Spectrometer E980C are presented in Table 5.

The hardness of the samples was determined using Brinell hardness tester carried out under a load of 60N and a dwell time of 10 seconds. The impact energy of the samples was determined using a Charpy Impact Machine (specification). The results of the hardness and charpy impact test are graphically represented in Figs. 5 and 6 respectively.

The wear test was carried out on a 200 mm diameter surface 150 µm mesh emery paper mounted on pin-on-disc apparatus to investigate the dry sliding wear characteristic of grey cast Iron. Various wear parameters such as speed, time and load were varied during the experiment. Each sample was placed at 90mm diameter from the centre of emery paper during the test. The initial weight of the samples was measured before and after each test with a measuring electronic scale with 0.001 mg accuracy. Prior to weighing, the worn out samples were cleaned with wool soaked in acetone and wear particles on the emery paper intermittently removed by compressed dry air blower. After running through a fixed distance, the samples were removed, clean with acetone, dried, and weighed to determine the weight loss due to wear. The differences in weight measured before and after tests give the wear loss of the samples. A parameter referred to as wear coefficient used to define the wear severity was calculated using Equation 1. The wear test was carried out with variable sliding speed, time and load as shown in Table 1.

Table 1. Process Parameter for the wear test.

Levels	Speed (rpm)	Time (sec)	Load (N)	Wt% Mn
1	125	60	10	0.31
2	250	120	15	1.71

Experiments were conducted as per standard 1.8 orthogonal arrays, with a view to investigate which of the design parameters: speed, load and time most significantly affect the dry sliding wear from the selected combinations. Equation 1 was used to calculate the wear rate [5].

$$\text{wear rate} = \frac{\text{wear volume loss}}{\text{sliding distance} \cdot \text{applied load}} \quad (1)$$

Factorial design and linear regression methods is a common tools used in engineering analysis [6]. It

consists of data acquisition in a sequential and controlled manner and execution of the experiments in order to obtain information about the behaviour of a given process. Two levels of each of the four factors were used for the statistical analysis. The levels for the four factors are entered in Table 2 and the treatment combinations for the two levels and four factors are tabulated in Table 3.

Table 2. Design parameter for the wear process.

Factor	Name	Units	Low level (-)	High level (+)
A	Speed	rpm	125	250
B	Time	sec	60	120
C	Load	N	10	15
D	Mn	Wt%	0.31	1.71

Coded: (low level), +(upper level), 0(Base line)

Table 3. Design layout and response data for Wear study.

Standard order	Speed (A) rpm	Time (B) sec	Load (C) N	Wear rate at 0.31 % Mn	Wear rate at 1.71 % Mn
1	125	1	15	0.42	0.04
2	250	1	15	0.13	0.02
3	250	2	10	0.17	0.07
4	250	2	15	0.14	0.05
5	125	2	15	0.22	0.03
6	250	1	10	0.17	0.02
7	125	1	10	0.24	0.04
8	125	2	10	0.31	0.12

The model equation was obtained by representing the wear value by *W*, as function process parameters below:

$$W = f(A, B, C, D) \tag{2}$$

Equation 2, represents the wear as a function of Sliding speed (A), time (B) and, load (C), and (D) is the percentage Ferro manganese addition.

The model selected includes the effects of main variables first-order and second-order interactions of variables. Hence the general model is represented as:

$$W = \beta_0 + \beta_1A + \beta_2B + \beta_3C + \beta_4D + \beta_5AB + \beta_6AC + \beta_7AD + \beta_8BC + \beta_9BD + \beta_{10}CD + \beta_{11}ABC + \beta_{12}ABD + \beta_{13}ACD + \beta_{14}BCD + \beta_{15}ABCD \tag{3}$$

Where β_0 , is average response of *W* and $\beta_1, \beta_2, \beta_3, \beta_4, \beta_5, \beta_6, \beta_7, \beta_8, \beta_9, \beta_{10}, \beta_{11}, \beta_{12}, \beta_{13}, \beta_{14}, \beta_{15}$ are coefficients associated with each variable A,B, C and interaction.

Scanning Electron Microscope (SEM), model EVO-MA10 L_aB₆ Analytical VP-SEM was used to determine the morphology of the worn out samples at 20 kV. The results of the SEM micrographs are presented in Plates 1 and 2. The microstructures were examined immediately after the samples were washed, cleaned adequately and air dried.

3. RESULTS AND DISCUSSION

From Fig. 1, it can be seen that as the manganese content increases, the wear coefficient decreases with increasing load and the samples with the lowest manganese additions gave the highest wear coefficient (0.45mm³/Nm).

From Figs. 2 and 3, under varying applied load and sliding speed, the wear coefficient behaves in a similar manner to Fig. 1. It appears from Fig. 3, which as the speed is varied, the change in the wear coefficient is most pronounced compared to changes observed when process parameters such are time and applied load are varied. This observation is indicative of the fact that changes in speed are the most influential wear parameter under these set test conditions.

The transition in the wear behaviour observed from Figs. 1 and 2 occurs at low speed 125rpm and heavy load. This is believed to be the result of the voids created between the rough surface of the emery paper and the samples at the beginning of each wear test on the spin on disc equipment. Substituting the coded values of the variables for any experimental condition in Eqn. (3), the wear rate of grey cast iron and the grey cast iron having different additions of manganese can be calculated. The final linear regression equation for the wear rate of the grey cast iron with different additions of manganese when tested against a pin on disc set up can be expressed as follows:

$$W = 0.16 - 0.028A + 0.028C - 0.098D + 0.050AB + 0.025AC + 0.040AD \tag{4}$$

The regression coefficients associated with the variable i.e., sliding speed is positive which indicate that wear rate increases with increasing sliding speed. In line with above explanation, the effectiveness of material removal increases with increasing sliding speed due to increasing depth of indentation and cutting efficiency.

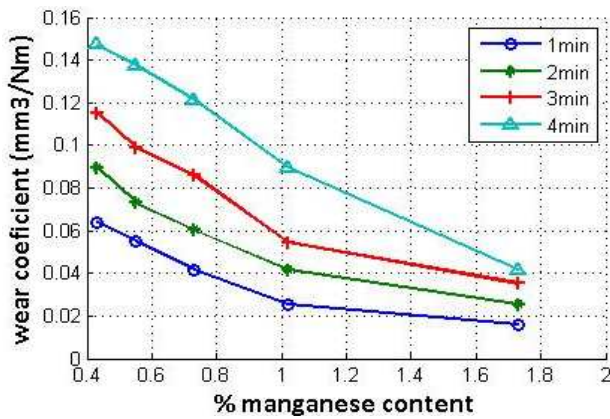


Fig. 1. Change in wear coefficient with increasing time.

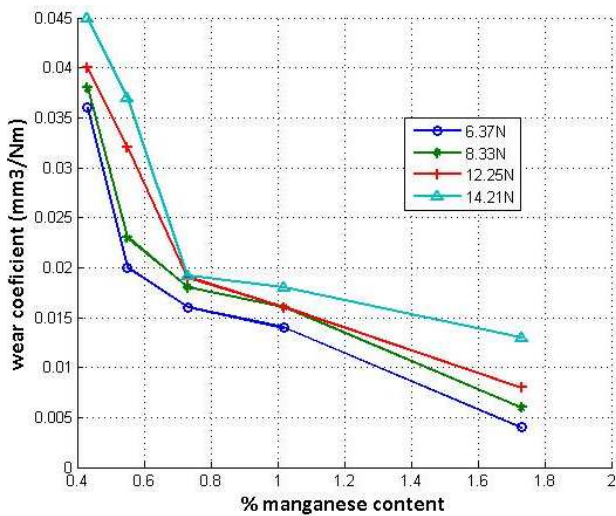


Fig. 2. Change in wear coefficient with increasing load.

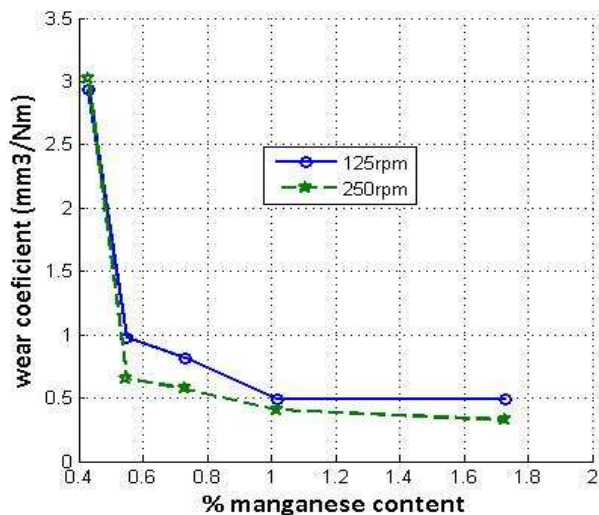


Fig. 3. Change in wear coefficient with increasing speed.

The analysis of variance was used to investigate which design parameters significantly affect the wear characteristic. It was accomplished by separating the total variability of the wear result, which is measured by sum of the squared deviations from the wear rate obtained, into

contributions by each of the design parameters and the errors.

Table 4. Comparison of actual and predicted model values result.

Source	Sum of Squares	DF	Mean Square	F Value	Prob >F
Model	0.13	6	0.021	419.83	0.0373
A	6.050E-003	1	6.050E-003	121.00	0.0577
C	6.050E-003	1	6.050E-003	121.00	0.0577
D	0.076	1	0.076	1521.00	0.0163
AB	0.020	1	0.020	400.00	0.0318
AC	5.000E-003	1	5.000E-003	100.00	0.0635
AD	0.013	1	0.013	256.00	0.0397
Residual	5.000E-003	1	5.000E-003		
Cor Tota	0.13	7			

Examination of the calculated values of Fishers (F) (Table 4) for all control factors also showed a very high influence of manganese additions, applied load and sliding speed on wear rate of grey cast iron (Table 3). From Table 3, it can be observed that the additions of manganese to grey cast iron have the most significant effect on wear, followed by load and sliding speed respectively. Time has no significant effect. From this statistical analysis, the manganese additions, sliding speed and load all affect the wear behaviour of low alloy grey cast iron.

The interactions effect of sliding speed-time also shows significant effect on the grey cast iron with manganese. The model F-value of 419.83 implies the model is significant. There is only a 3.73 % chance that a “Model F-Value” this large could occur due to noise. Value of “Prob F” less than 0.0500 indicate model terms are significant. This model can be used to navigate the design space.

3.1 Microstructure result

Plate 1 is the micrograph of the grey cast Iron sample without deliberate additions of Ferro manganese addition. It is the sample with the lowest percentage of manganese. The structure represents a typical grey cast iron which contains large volume of soft graphite flakes embedded in the matrix of the microstructure. Therefore, it is also characteristically not too hard (235HRB).

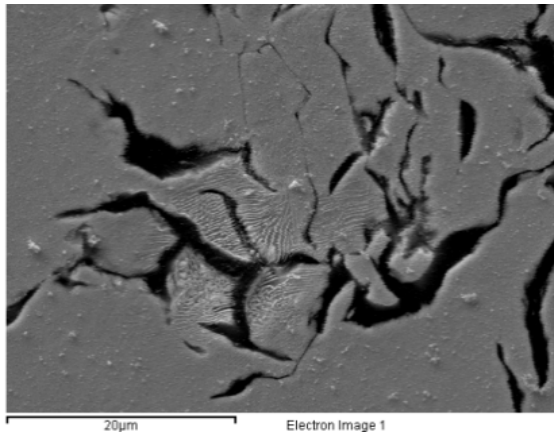


Plate 1. SEM Micrographs of grey cast iron with Manganese additions 0.24 % Mn.

Plate 2a, b and c represent grey cast Iron with 0.47 % Mn, 0.73 % Mn and 1.71 % Mn additions respectively.

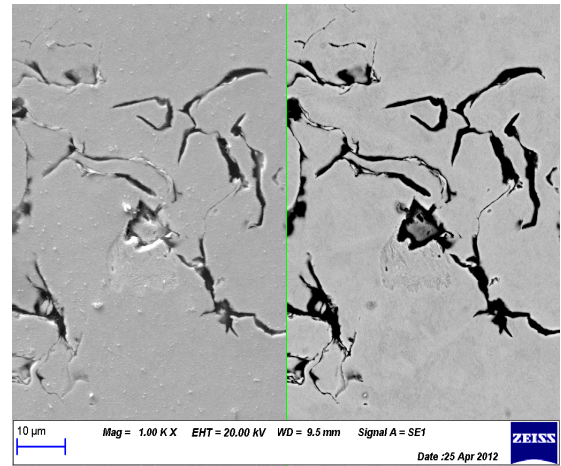
It can be seen from Plate 2a, b and c that the volume of the soft graphite flakes has been substituted for hard carbide (FeMn)₃C reduced as the manganese addition increases. This may have been responsible for the slight increase in hardness with a corresponding increase in toughness as indicated in Figure 6. Another factor which may have contributed to low hardness is the decrease in the sulphur content as the percentage manganese increase in accordance to the reaction in Equation 5. This observation agreed with the decrease sulphur content in the spectrometer results in Table 5.



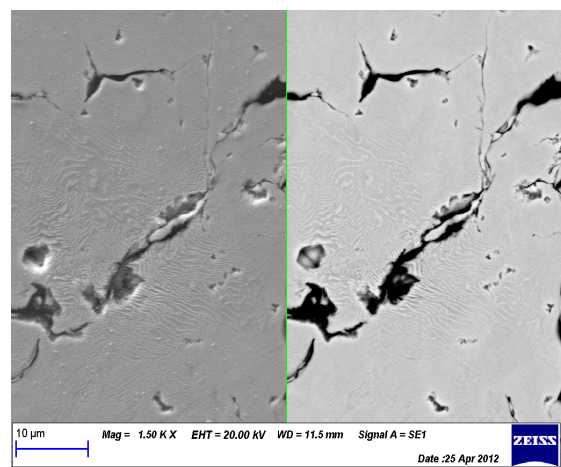
Table 5. Chemical composition of experimental grey cast iron (wt %).

	C (%)	Si (%)	Mn (%)	P (%)	S (%)	Fe (%)
Batch 1	3.32	1.90	0.31	0.12	0.11	94.2
Batch 2	3.30	1.94	0.43	0.11	0.09	94.0
Batch 3	3.26	2.00	0.73	0.08	0.06	93.8
Batch 4	3.24	2.10	1.02	0.09	0.05	93.4
Batch 5	3.20	2.07	1.71	0.09	0.05	92.8

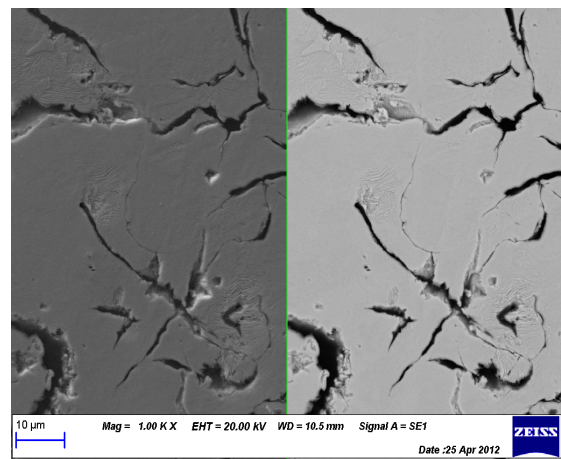
The Micrographs in Plate 2 a-b shows similar trend to Plate 1 described above. There is reduction in graphite flake and increase toughness due to increase volume fraction of (FeMn)₃C carbide at the expense of soft graphite flakes. This is followed with a corresponding increase in the impact energy in Joules Figure 6. The combination of these factors is responsible for improve wear rate under varied time and increase load application as shown in Figs. 2 and 3 respectively.



a)



b)



c)

Plate 2. SEM Micrographs of grey cast iron with Manganese addition: (a) 0.46 % Mn, (b) 0.73 % Mn, (c) 1.71 % Mn.

The carbon equivalent is a parameter that is often used to predict carbide formation, in grey cast Iron. The carbon equivalent of the grey cast iron samples were calculated according to [4]. The formula used is presented in Equation 6.

$$CE = \%C + 0.3(\%Si) + 0.33(\%P) - 0.027(\%Mn) + 0.4(\%S) \quad (6)$$

Higher (CE) is indicative of faster solidification in the mould and to a larger extent formation of large volume of hard carbide Fe₃C. This type of carbide is responsible for brittleness in gray cast iron.

From Fig. 4, it can be seen that as the percentage of manganese increases, the carbon equivalent (CE) decrease gradually up to CE = 3.90, remain flat between (0.73 to 1.02)% Mn and then decreased further. This explains how partly the gray cast Iron sacrifices its high hardness value for toughness and subsequently improved wear resistance. It appears that between (0.73 - 1.102)% Mn, represent the lower and upper limits of the solid solubility of Manganese in gray cast Iron. The microstructure at within the range can be said to be more stable and ideal for optimum toughness and good wear resistance. The reduction in the volume of soft graphite flakes and the strengthening effect of tough carbide (FeMn)₃C combines to fortify the matrix and help improve the wear resistance of gray cast iron [16].

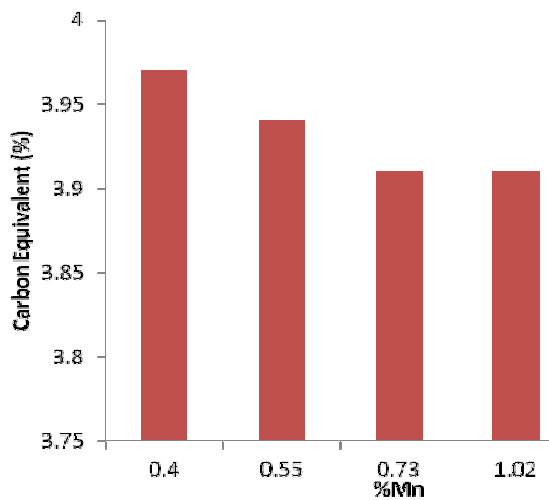


Fig. 4. (CE) of the grey cast iron compared with eutectic composition.

The changes in hardness as the manganese content increase in the grey cast iron are presented in Fig. 5. Decreasing trend in hardness with increase in manganese content was observed. The alloy with 1.71 % manganese content shows lowest hardness value.

The difference in hardness between the alloys depends on the amount of hard alloy carbide formed and on the volume and distribution of soft

flake graphite. From Plate 2a-c, it can be seen from the Scanning Electron Microscope results that the volume and distribution of soft flake graphite decreases with increase in manganese addition in the sample. This explains the decreasing trend in hardness as observed in Fig. 5. Also, the micro alloying additives readily form strong carbides in the matrix which tend to refine the grain size during solidification. This fine distribution of the carbides also enhances the wear resistance [11].

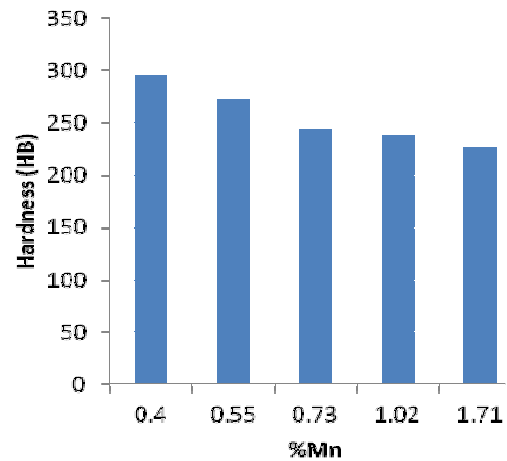


Fig. 5. Hardness of the different compositions of grey cast iron.

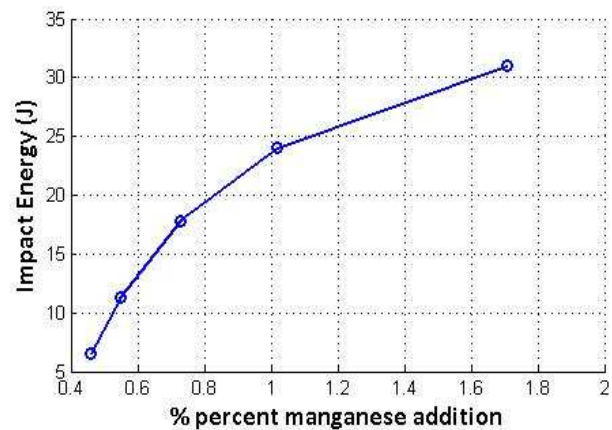


Fig. 6. Change in impact energy with increasing time.

4. CONCLUSIONS

From the results of the investigation the following conclusions are made:

1. The wear coefficient with respect to increasing load, speed and time decreases with increasing manganese additions for the low alloy grey cast iron.
2. The improved wear resistance of the samples with increasing manganese

additions is due to the formation of hard carbide phase within the matrix structure of the low alloy grey cast irons.

3. Increasing manganese additions leads to decrease CE. This will guarantee lower mould solidification resulting to significant reduction in the formation of hard and brittle inter-metallic second phase Fe₃C and improved toughness.
4. The dominant effect on wear resistance is the morphology and size of the carbide.
5. Factorial design of the experiment can be successfully employed to describe the wear behaviour of low alloy gray cast Iron and the developed linear equation models can be used in predicting the wear rate of the materials within the set experimental conditions.
6. The main effects of manganese additions, load and speed variables are more pronounced on the wear behaviour of the low alloy grey cast iron when compare with main effect of time.
7. The sliding speed-time interactions effect gave the most significant effect on the low alloy grey cast iron.

REFERENCES

- [1] W. Zhou, H. Zhu, D. Zheng, H. Zheng, Q. Hua, Q. Zhai: *Niobium alloying effect in high carbon equivalent grey cast iron*, China Foundry, Vol. 8, No. 1, pp. 36-40, 2011.
- [2] C. Meric, S. Sahin, B. Backir, N. Koksali: *Investigation of the boronizing effect on the abrasive wear behavior in cast irons*, Journal of Materials and Design, Vol. 27, No. 9, pp. 751-757, 2006.
- [3] K. Edalati, F. Akhlaghi, M. Nili-Ahmadabadi: *Influence of Si and FeSi addition on the characteristics of gray cast iron melts poured at different temperatures*, Journal of Materials Processing Technology, Vol. 160, No. 2, pp. 183-187, 2005.
- [4] V. Rudnev: *Handbook of Induction heating*, CRC Press, 2003.
- [5] V.S. Aigbodion, S.B. Hassan, J.O. Agunsoye: *Effect of ash reinforcement on dry sliding wear behaviour of polymer matrix composites*, Journal of Materials and Design, Vol. 33, pp. 322-327, 2011.
- [6] V.S. Aigbodion, S.B. Hassan: *Experimental correlation between wear rate and wear parameter of Al-Cu-Mg/Bagasse ash particulate composite*, Journal of Materials and Design, Vol. 31, pp. 2177-2180, 2010.
- [7] I. Miller, J. Freund: *Probability and Statistics for engineers*, Prentice Hall India Ltd, India, pp. 125-214, 2001.
- [8] T. Alp, A. Wazzan, F. Yilmaz: *Microstructure-property relationships in cast irons*, The Arabian Journal for Science and Engineering, Vol. 30, No. 2b, pp. 163-175, 2005.
- [9] O. Aponbiede and N.M. Okelekwe: *The effect of chloride salt on the mechanical properties of grey cast*, J. of Emerging Trends in Eng. and Applied Sci., Vol. 2, No. 2, pp. 256-259, 2011.
- [10] Park Ik-Min and K.S. Shin: *Microstructure and wear properties of low-alloy phosphoric gray cast irons*, Metals and Materials International, Vol. 1, pp. 63-70, 1995.
- [11] Aravind Vadiraj, M. Kamaraj, V.S. Sreenivasan: *Wear and friction behavior of alloyed gray cast iron with solid lubricants under boundary lubrication*, Tribology International, Vol. 44, pp. 1168-1173, 2011.
- [12] W. Xu, M. Ferry, Y. Wang: *Influence of alloying elements on as-cast micro-structure and strength of gray iron*, Materials Science and Engineering: A, Vol. 390, No. 1-2, pp. 326-33, 2005.
- [13] P. Atanda, G. Oluwadare and O. Oluwole: *Effect of Silicon Content and Shake-Out Time on Hardness and Grain Size Properties of GL 250 Cast Iron*, J. of Minerals & Mat. Characterization & Eng., Vol. 10, No. 3, pp. 257-266, 2011.
- [14] Alan Alderson: *The Influence of Manganese and Sulphur on the Structure and Mechanical Properties of Grey Cast Iron*, The free library, Science and technology, general community 2010.
- [15] L.B. Singh: *Improvement in properties of grey iron after boron additions*, in: *Transactions of 57th IFC 2009*, February 13-15, Kolkata, India, pp. 166-171, 2009.
- [16] J.O. Agunsoye and A.A. Ayeni: *Effect of Heat Treatment on the Abrasive Wear Behaviour of High Chromium Iron under Dry Sliding Condition*, Tribology in Industry, Vol. 34, No. 2, pp. 82-91, 2012.
- [17] A.D. Sarkar: *Mould and core material for steel*, Pergamon press, London, pp. 5-21, 1967.